

Study of Gas-to-Liquid Mass Transfer by Dynamic Methods in Trickle Beds

A. Goenaga, J. M. Smith,
B. J. McCoy

Department of Chemical Engineering
University of California
Davis, CA 95616

Mass transfer in trickle-bed reactors plays an important role in overall performance (Shah, 1979; Ramachandran and Chaudhari, 1985). Several studies have been published on the liquid-side mass transfer coefficient (Goto et al., 1975; Tan and Smith, 1982; Fukushima and Kusaka, 1977; Turek and Lange, 1981). Goto et al. (1975) studied gas-side mass transfer coefficients for desorption of naphthalene dissolved in water into air. Mata (1980) performed steady-state experiments with sulfur dioxide in water to measure mass transfer. Eroglu and Dogu (1983) applied moment analysis to pulse-response experiments similar to the ones described in this work, using cylindrical pellets of a larger size.

Mass transfer data can be obtained with either steady state or dynamic techniques, although the latter have seldom been used. Dynamic experiments are often easier to perform and provide more information (Burghardt and Smith, 1979). The dynamic method is illustrated here by analyzing pulse-response experiments for SO_2 in inert N_2 flowing cocurrently with water downward through a packed bed of glass spheres. To obtain overall gas-to-liquid mass transfer coefficients, only zero moments are needed. For the very soluble gas-liquid pair, $\text{SO}_2\text{--H}_2\text{O}$, axial dispersion in the liquid could be neglected, simplifying the data analysis. For transitions between flow regimes our results can be interpreted by allowing mass transfer coefficients to depend on gas velocity to a power greater than unity.

Reproducibility is a major issue in experiments with trickle beds, for dynamic as well as for steady-state methods. In our experiments the gas-liquid disengaging section of the apparatus had a large effect. Following the procedure of Ramachandran and Smith (1979), we derived expressions for a multisectioned trickle bed, and used these new results to account for the mass transfer in the lower section of our apparatus where the gas and liquid are disengaged.

Experimental Apparatus

The reactor (Figure 1) was a 0.3 m long glass tube of 1.6×10^{-2} m ID. The liquid was introduced to the reactor through a

movable distributor consisting of 12 (1×10^{-3} m ID, 5×10^{-3} m long) stainless steel capillary tubes located uniformly across the reactor cross-sectional area. The outlet of the capillary tubes was directly in contact with the bed packing, which was supported by a 60-mesh stainless steel screen. This was the same liquid distributor utilized by Tan and Smith (1982). Spherical glass beads ($d_p = 8.13 \times 10^{-4}$ m, 16–20 Tyler mesh), constituted the packing with $d_t/d_p > 18$, thus satisfying the criterion for uniform liquid distribution (Herskowitz and Smith, 1978).

At the reactor outlet, gas and liquid streams were separated by the same device used by Tan and Smith (1982) and by Seirafi and Smith (1980). About 2.5×10^{-6} m³/s of the gas stream was accurately measured and directed to the detector for analysis. The detector consisted of a thermal conductivity cell in a Varian Chromatograph, Model 90-P, with the column replaced by a $1/4$ inch stainless steel tube to connect the gas chromatograph. The small amount of water vapor in the gas stream was determined to have no effect on the thermal conductivity measurement of SO_2 concentration. A variable-speed strip-chart recorder printed the output signal from the detector. All runs were made at 25°C and atmospheric pressure.

At the reactor entrance, a Varian six-port valve allowed pulses of SO_2 to be introduced from a 4.0×10^{-6} m³ sample loop. The SO_2 and N_2 gases (from Liquid Carbonic Co.) were 99.99% pure. Distilled water was fed to the reactor by a variable-speed, positive displacement pump. All tubing and fittings were of Tygon or stainless steel.

Theory

Ramachandran and Smith (1979) have presented the governing differential equations for the trickle bed at constant temperature, with no transverse concentration gradients, the gas moving in plug flow, and an axial dispersion model for liquid flow. A similar model, with calculations restricted to zero moments, is proposed in this paper. When the gas tracer is highly soluble, as in our experiments, it is readily demonstrated that the effect of liquid axial dispersion vanishes in the expres-

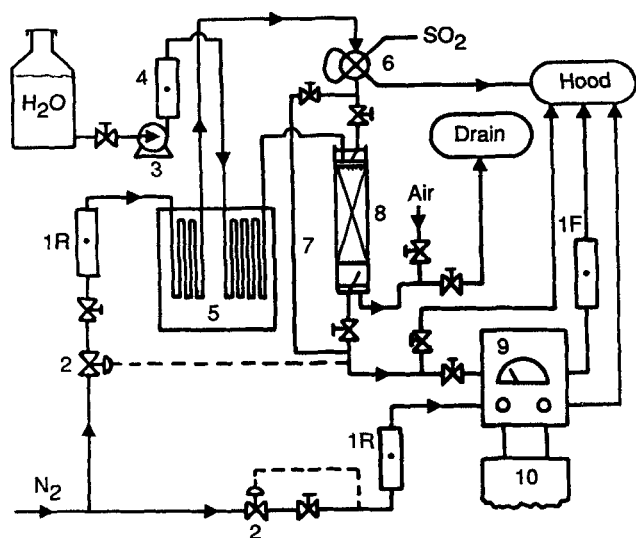


Figure 1. Experimental apparatus.

- | | |
|------------------------------|------------------------|
| 1R. gas flowmeters | 6. injection valve |
| 1F. soap film flowmeter | 7. bypass circuit |
| 2. flow controllers | 8. trickle-bed reactor |
| 3. water pump | 9. detector |
| 4. liquid flowmeter | 10. recorder |
| 5. constant temperature bath | |

sion of the zero moment. We extend the analysis to include multiple sections, including the gas-liquid disengaging section, for the case of negligible axial dispersion of liquid. For the gas the Peclet number is large, so that the plug-flow assumption is valid (Goto and Smith, 1975). As the zero moment is the limit of the Laplace transform when the transform parameter approaches zero, this limit can be applied before solving the ordinary differential equation in the Laplace-transform domain. By this procedure the dimensionless zero moment for tracer in the gas reduces to the following expression for a single section of packed bed,

$$m_{0,G} = \int_0^\infty c_G(t) dt \bigg/ \int_0^\infty c_{G,0}(t) dt = \exp(-\alpha) \quad (1)$$

Experimental values for $m_{0,G}$ are evaluated from the integrals using the measured response curve. The last member of Eq. 1 is obtained from the model equations and depends on $K_L a_L$ since

$$\alpha = K_L a_L L / H u_G \quad (2)$$

where

$$1/K_L a_L = 1/k_L a_L + 1/H k_G a_L \quad (3)$$

Henry's law constant, H is small ($H = 0.0121$ at 298°C according to Komiyama and Smith, 1975) for the very soluble SO_2 gas in water. Because the diffusivity in the gas phase is about 10^4 times that in the liquid phase, k_g is expected to be about 10^2 times k_L . This makes $k_L a_L$ comparable in magnitude to $H k_g a_L$. An example in McCabe et al. (1985) likewise shows that gas and liquid mass transfer resistances both contribute to the overall resistance for SO_2 absorption in a packed column.

Mass transfer occurs in the section of the trickle bed where the gas and liquid are disengaged, as well as in the packed bed.

We treat this section by modeling it in the same manner as the packed bed, but with separate parameters, indicated by subscripts 2 for the disengaging section and 1 for the packed bed. The same partial differential mass balance equations, neglecting axial dispersion, are written for the gas-liquid disengaging section, with the appropriate boundary conditions. The zero-moment equations for the gas and liquid streams, for the general case when tracer is introduced in both the liquid and gas streams, are

$$(1/m'_G) \int_0^\infty c_G(t) dt = m_{0,G,\text{all}} = (\beta + E)/(1 + \beta) + [m'_L/m'_G](1 - E)H/(1 + \beta) \quad (4)$$

$$(1/m'_G) \int_0^\infty c_L(t) dt = m_{0,L,\text{all}} = \beta(1 - E)/(1 + \beta) + [m'_L/m'_G](1 + \beta E)H/(1 + \beta) \quad (5)$$

where

$$m'_L = \int_0^\infty c_{L,0}(t) dt, \quad m'_G = \int_0^\infty c_{G,0}(t) dt, \quad (6)$$

and

$$E = \exp\{-[\alpha_2(1 - s) + \alpha_1 s](1 + \beta)\} \quad (7)$$

The expressions for the dimensional zero moments in Eqs. 4 and 5 are easily obtained for special cases when the input pulse is either completely in the gas or completely in the liquid, i.e., $m'_L = 0$ or $m'_G = 0$, respectively.

The extension to the case of n sections of the trickle bed can be shown to yield the same moment expressions as above, Eqs. 4–6, but with

$$E = \exp[-(1 + \beta)\Gamma] \quad (8)$$

in terms of

$$\Gamma = \sum_{i=1}^n \alpha_i L_i / L \quad (9)$$

It is important to recognize that the influence of the length and mass transfer capacity of one or more sections appears not linearly, but exponentially in the zero moment.

For an infinitely long reactor, the gas and liquid streams are in equilibrium and Eqs. 4 and 5 reduce to

$$m_{0,G,\text{eq}} = m_{0,L,\text{eq}} = \beta/(\beta + 1) + H m'_L/m'_G \quad (10)$$

For the case when the input pulse is fed only to the gas stream ($m'_L = 0$) the moment responses, from Eqs. 4 and 5, are given by

$$m_{0,G,\text{all}} = (\beta + E)/(1 + \beta) \quad (11)$$

$$m_{0,L,\text{all}} = \beta(1 - E)/(1 + \beta) \quad (12)$$

These two equations are not independent since a global mass balance of the absorbable tracer dictates that

$$m_{0,G,\text{all}} = m_{0,L,\text{all}}/\beta = 1 \quad (13)$$

so that, in principle, concentration measurements are necessary in one phase only.

Focusing on the gas phase zero moment, we can solve for α_1 in Eqs. 4 and 7 obtaining

$$\alpha_1 = -B/(1 + \beta)s - \alpha_2(1/s - 1) \quad (14)$$

where

$$B = \ln [(1 + \beta)m_{0,G,\text{all}} - \beta] \quad (15)$$

It is convenient, when $s = 1$, to let

$$\alpha_{1,F} = -B/(1 + \beta) = L(K_L a_L)_{\text{all}}/Hu_G \quad (16)$$

In fact, $\alpha_{1,F}$ would be the "false" mass transfer group one would obtain if the presence of the second section were not considered. In terms of Eq. 16, Eq. 14 becomes

$$\alpha_1 = \alpha_{1,F}/s - \alpha_2(1/s - 1) \quad (17)$$

Next we set $s = 0$ in Eq. 7 and substitute into Eq. 4 with $m'_L = 0$. The result is

$$m_{0,G,2} = [\beta + \exp - \alpha_2(1 + \beta)]/(1 + \beta) \quad (18)$$

which represents the amount of absorption that would take place in a reactor of length L , constituted only by section 2, the disengaging section. Solving from Eq. 18 we get

$$\alpha_2 = -(1 + \beta)^{-1} \ln [(1 + \beta)m_{0,G,2} - \beta] \\ = L(K_L a_L)_2/Hu_G \quad (19)$$

so that for a reactor of length $L - L_1 = L(1 - s)$,

$$\alpha_{2,0} = \alpha_2(1 - s) \quad (20)$$

Then Eq. 17 becomes

$$\alpha_1 = (\alpha_{1,F} - \alpha_{2,0})/s \quad (21)$$

which is our working equation. As a check on the solution, we may substitute into Eq. 21 the corresponding definitions for α_1 , $\alpha_{1,F}$, and $\alpha_{2,0}$. This gives

$$s(K_L a_L)_1 + (1 - s)(K_L a_L)_2 = (K_L a_L)_{\text{all}} \quad (22)$$

which is the steady-state result relating mass transfer coefficients for the two sections.

The equations suggest the following experimental plan:

- Evaluate the mass transfer capacity of section 2 by measuring the zero moment for this section alone. Use Eq. 20 to determine $\alpha_{2,0}$
- Evaluate the overall mass transfer rate for combined sections 1 and 2 by measuring the zero moment. Use Eq. 16 to determine $\alpha_{1,F}$
- Determine the bed mass transfer coefficient through Eq. 21

Results

Measurements for the entire trickle-bed system were made with two lengths of packed beds, 5.0 and 7.5 cm. To determine

the zero moment for the gas-liquid disengaging section alone, the reactor was emptied except for three to four layers of glass beads. The distributor was lowered onto the top of these layers to simulate the hydrodynamics at the exit of the reactor. The absorption of SO_2 in the disengaging end section was significant as indicated by the low value of the zero moment compared to unity.

The measured zero moments are given in Table 1 for the end section, the 5.0 cm bed plus the end section, and for the 7.5 cm bed plus the end section. The moments are average values with a variation (difference between extreme values divided by the average) of less than 9% for the disengaging end section only. Also presented in Table 1 are the mass-transfer groups, $\alpha_{2,0}$ and $\alpha_{1,F}$ for the 5.0 and 7.5 cm beds, respectively. The zero moment measurements showed a 15% variation causing a 16% variation in the mass transfer group $\alpha_{1,F}$. Replication experiments made on different days yielded differences in moments of less than 10%, resulting in a difference in mass transfer coefficients of 20%. The equilibrium values of the moments (at $\alpha = \infty$) are also tabulated, showing that $m_{0,G}$ decreases to its minimum as α increases.

Mass transfer coefficients, calculated according to Eq. 21, for the 7.5 cm bed either agreed with or were larger than those for the 5.0 cm bed. The experiments for the 7.5 cm bed were closer to equilibrium conditions, due to increased contact between gas and liquid. For operations close to equilibrium conditions, small changes in the zero moment cause relatively large changes in the mass transfer parameter, α . A linear regression of the data with the logarithmic form of the correlating equation,

$$K_L a_L/H = au_G^b u_L^c \quad (23)$$

yielded constants a , b , and c with a relatively large standard deviation. Some of the scatter in the data is due to the effect of the disengaging section, as can be shown by an error propagation analysis.

Table 1. Moments and Mass Transfer Groups for Values of Gas Velocity, u_G , and Liquid Velocity, u_L

$U_G U_L$	0.675 cm/s		1.26 cm/s		1.90 cm/s		2.61 cm/s	
cm/s	$m_{0,G}$	α	$m_{0,G}$	α	$m_{0,G}$	α	$m_{0,G}$	α
3.28	0.338	1.14	0.237	1.52	0.150	2.01	0.102	2.40
	0.204	1.75	0.113	2.39	0.086	2.65	0.059	3.09
	0.193	1.82	—	—	0.078	2.77	0.039	3.67
5.26	0.056	∞	0.031	∞	0.021	∞	0.015	∞
	0.464	0.81	0.373	1.03	0.194	1.73	0.192	1.71
	0.316	1.26	0.153	2.11	0.118	2.34	0.097	2.54
7.84	0.254	1.55	—	—	0.107	2.48	0.040	4.06
	0.086	∞	0.048	∞	0.033	∞	0.024	∞
	0.465	0.83	0.424	0.90	0.264	1.40	0.262	1.40
11.0	0.356	1.16	0.193	1.89	0.146	2.20	0.123	2.31
	0.249	1.70	0.137	2.44	0.079	3.25	0.058	3.59
	0.123	∞	0.070	∞	0.048	∞	0.035	∞
	0.493	0.78	0.390	1.02	0.363	1.07	0.272	1.38
	0.369	1.18	0.245	1.63	0.137	2.40	0.127	2.38
	0.241	2.00	0.138	2.77	0.107	2.92	0.068	3.69
	0.165	∞	0.096	∞	0.066	∞	0.049	∞

*The four entries of moments in the first column at each gas and liquid flow rate are the zero moments for: 1) the end section; 2) the 5.0 cm bed plus the end section; 3) the 7.5 cm bed plus the end section; and 4) the equilibrium value. The first three of α entries in the second column at each flow rate are the mass transfer groups $\alpha_{2,0}$, $\alpha_{1,F}$ for the 5.0 cm bed, and $\alpha_{1,F}$ for the 7.5 cm bed. The equilibrium values of the moments are paired with $\alpha = \infty$.

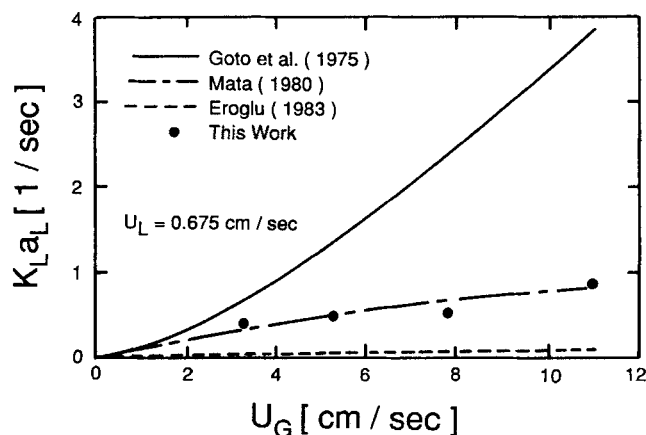


Figure 2. Correlations of the overall gas-to-liquid mass transfer coefficient, $K_L a_L$, as a function of the gas velocity, u_G , at liquid velocity $u_L = 0.675$ cm/s.

The regression showed that the mass transfer coefficient depends on the gas flow rate to a power (b) greater than unity. This dependency implies that at a higher gas flow rate one could obtain better fractional removal of gas solute for a given size of reactor. Goto et al. (1975) also reported an increase in the gas-side coefficient to a power greater than unity (~ 1.45) for their experiments. For liquid-side mass transfer coefficients, a similar kind of functionality was found by Ufford and Perona (1973), Fukushima and Kusaka (1977a), and Sylvester and Pitayagulsarn (1975).

Bird et al. (1960) show that in the transition region from laminar to turbulent flow in a pipe, the heat transfer coefficient depends on a power greater than that for the fluid velocity. Chou et al. (1979) also reported that in the transition region from gas-continuous to pulsing flow, the liquid-solid mass transfer coefficient increased sharply, in a manner proportional to u_L^3 . These facts led us to believe that a flow transition could explain the behaviour of our data. Although pulsing flow was not observed, the flow map of Tosun (1984) indicates that a transition from gas-continuous (trickling) to pulsing flow should occur in this range of gas and liquid velocities. The boundaries between flow regimes are not sharp, and visually distinguishing the transition can be difficult.

Figure 2 shows a comparison of our results for the 5.0 cm bed, and those of other workers for the liquid velocity 0.675 cm/s. The results of Goto et al. (1975) have a stronger gas velocity dependence, while those of Eroglu and Dogu (1983) have a weaker velocity dependence. Our correlation of the mass transfer coefficient agrees best with Mata (1980).

Table 2. Correlation Parameters for Eq. 25, $K_L a_L = du_G^e$ *

u_L	d	e
0.675	2.42×10^{-3}	0.589
1.26	3.40×10^{-3}	0.740
1.90	6.30×10^{-4}	1.61
2.61	8.00×10^{-4}	1.49

* $K_L a_L$ in 1/s, u_G in cm/s at four values of liquid velocity and for the 5.0 cm trickle bed

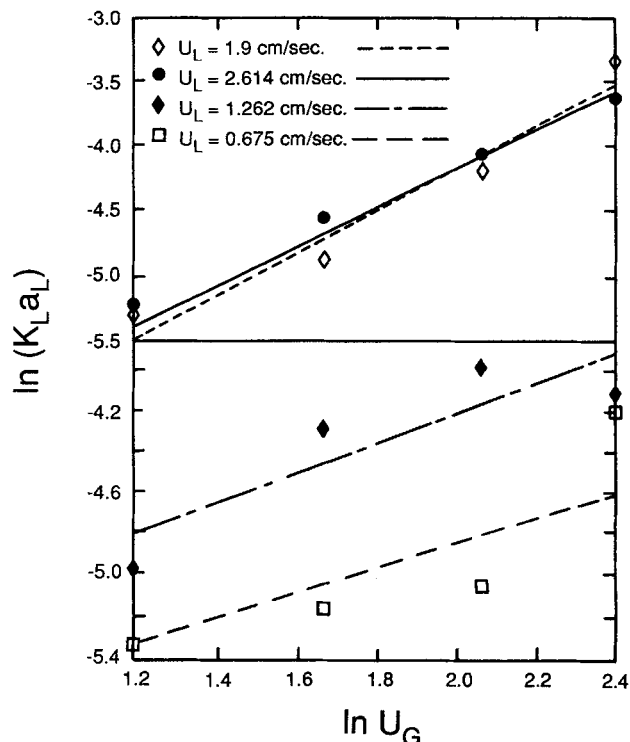


Figure 3. Mass transfer coefficient according to Eq. 24 for $u_L = 0.675, 1.262, 1.900$ and 2.614 cm/s.

At higher liquid flow rates the agreement of the correlation and the experimental results was better than at lower liquid flow rates. This suggested that the liquid velocity effect had not been determined as accurately as possible. Thus the data were organized into sets of constant liquid flow rate and correlated with the equation

$$K_L a_L = du_G^e \quad (24)$$

This fit showed less scatter of the data than did Eq. 23. The values of the parameters d and e are given in Table 2, and the mass transfer coefficient is plotted as a function of gas velocity in Figure 3. Each experimental point in Figure 3 is an average of up to nine observations. The interesting feature of Table 2 is the sharp difference between the parameters d and e for liquid velocity between $u_L = 1.26$ and $u_L = 1.90$. According to Tosun (1984), the transition of trickling to pulsing flow should occur between these liquid flow rates. This is further evidence that the mass transfer is dependent upon the flow regime.

Acknowledgement

This research was supported in part by a grant from Chevron Research Company. The assistance of Dr. Jorge Gabitto, and thoughtful comments by Prof. Peter Harriott are gratefully acknowledged.

Notation

- a_L = gas-liquid mass transfer area per unit column volume, m^2/m^3
- B = quantity defined by Eq. 15
- c_G = concentration of tracer in the gas phase, mol/m^3
- $c_{G,0}(t)$ = concentration of tracer input in the gas feed, mol/m^3
- $c_{G,1}$ = exit concentration from section 1, mol/m^3

c_G = exit concentration from reactor, mol/m³
 c_L = concentration of tracer in the liquid, mol/m³
 $c_{L0}(t)$ = concentration of tracer in the liquid at entrance, mol/m³
 c_L = exit liquid concentration from reactor, mol/m³
 d_p = particle diameter, m
 d_r = reactor column diameter, m
 H = Henry's law solubility constant
 k_G = gas film mass transfer coefficient, m/s
 k_L = liquid film mass transfer coefficient, m/s
 $\left. \begin{matrix} (K_L a_L)_1 \\ (K_L a_L)_2 \\ (K_L a_L)_{all} \end{matrix} \right\}$ = mass transfer coefficients for sections 1, 2 and overall, L/s
 L = total length of the column, m
 L_i = length of section i of the trickle-bed, m
 m_0 = dimensionless zero moment, defined by Eq. 1
 s = dimensionless length L_i/L
 t = time, s
 u_G = superficial gas velocity, m/s
 u_L = superficial liquid velocity, m/s
 m'_L, m'_G = dimensional moments for inlet liquid or gas, Eq. 6, mol s/m³
 $m_{0,G}$ = dimensionless zero moment for tracer in the gas for single section of packed bed, Eq. 1
 $m_{0,G,2}$ = dimensionless zero moment for tracer in the gas for disengaging section, Eq. 18

Greek letters

$\alpha = [(K_L a_L)L]/Hu_G$
 $\alpha_1 = [(K_L a_L)_1 L]/Hu_G$
 $\alpha_{1,F} = [(K_L a_L)_{all} L]/Hu_G$
 $\alpha_2 = [(K_L a_L)_2 L]/Hu_G$
 $\alpha_{2,0} = [(K_L a_L)_2 (L - L_1)]/Hu_G$
 $\alpha_i = [(K_L a_L)_i L]/Hu_G$
 $\beta = Hu_G/u_L$
 Γ = dimensionless quantity defined by Eq. 9

Literature Cited

- Bird, R. B., W. E. Stewart and E. N. Lightfoot, *Transport Phenomena*, 400, John Wiley, New York, (1960).
 Burghardt, A., and J. M. Smith, "Dynamic Response of a Single Catalyst Pellet," *Chem. Eng. Sci.*, **34**, 267 (1979).
 Chou, T. S., F. L. Worley, and D. Luss, "Local Particle-Liquid Mass Transfer Fluctuations in Mixed-Phase Cocurrent Downflow through

- a Fixed Bed in the Pulsing Regime," *Ind. Eng. Chem. Fund.*, **18**, 279 (1979).
 Eroglu, I., and T. Dogu, "Dynamic Analysis of a Trickle Bed Reactor by Moment Technique," *Chem. Eng. Sci.*, **38**, 801 (1983).
 Fukushima, S., and K. Kusaka, "Liquid Phase Volumetric and Mass Transfer Coefficient and Boundary of Hydrodynamic Flow Region in Packed Bed Column with Cocurrent Downward Flow," *J. Chem. Eng. Japan*, **10**, 468 (1977).
 Goto, S., and J. M. Smith, "Performance of Trickle-Bed Reactors," *AIChE J.*, **21**, No. 4, 714 (July, 1975).
 Goto, S., J. Levec, and J. M. Smith, "Trickle-Bed Oxidation Reactors," *Ind. Eng. Chem. Proc. Dev.*, **14**, 473 (1975).
 Herskowitz, S., and J. M. Smith, "Trickle-Bed Reactors: A Review," *AIChE J.*, **29**, 1 (Jan., 1983).
 Komiyama, H., and J. M. Smith, "Sulfur Dioxide Oxidation in Slurries of Activated Carbon. Part II. Mass Transfer Studies," *AIChE J.*, No. 4, 670 (July, 1975).
 Mata, A. R., *Mass Transfer and Reactor Studies in a Trickle Bed Reactor*, Ph.D. Thesis, U. of CA., Davis, (1980).
 McCabe, W. L., J. C. Smith, P. Harriott, *Unit Operations of Chemical Engineering*, 4th Ed., McGraw Hill (1985).
 Ramachandran, P. A., and J. M. Smith, "Dynamic Behavior of Trickle-Bed Reactors," *Chem. Eng. Sci.*, **34**, 75 (1979).
 Ramachandran, P. A., and R. V. Chaudhari, *Three Phase Catalytic Reactors*, Gordon and Breach, New York (1983).
 Seirafi, H. A., and J. M. Smith, "Mass Transfer and Adsorption in Liquid-Full and Trickle Beds," *AIChE J.*, **26**, No. 5, 711 (Sept., 1980).
 Shah, Y. T., *Gas-Liquid-Solid Reactor Design*, McGraw-Hill, New York, (1979).
 Sylvester, N. D., and P. Pitayagulsarn, "Mass Transfer for Two-Phase Cocurrent Downflow in a Packed Bed," *Ind. Eng. Chem. Proc. Des. Dev.*, **14**, 421 (1975).
 Tan, C. S., and J. M. Smith, "A Dynamic Method for Liquid-Particle Mass Transfer in Trickle-Beds," *AIChE J.*, **28**, No. 2, 190 (March, 1982).
 Tosun, G., "A Study of Cocurrent Downflow of Nonfoaming Gas-Liquid Systems in a Packed Bed. Part I. Flow Regimes: Search for a Generalized Flow Map," *Ind. Eng. Chem. Proc. Des. Dev.*, **23**, 29 (1984).
 Turek, F., and R. Lange, "Mass Transfer in Trickle-Bed Reactors at Low Reynolds Number," *Chem. Eng. Sci.*, **36**, 569 (1981).
 Ufford, R. C., and J. J. Perona, "Liquid Phase Mass Transfer with Cocurrent Downflow through Packed Towers," *AIChE J.*, **19**, No. 6, 1223 (Nov., 1973).

Manuscript received Feb. 19, 1988 and revision received Aug. 9, 1988.